METABOLISM AND BIOENERGETICS:

Disruption of Mitochondrial β-Oxidation of Unsaturated Fatty Acids in the 3,2- *trans* -Enoyl-CoA Isomerase-deficient Mouse

Uwe Janssen and Wilhelm Stoffel

J. Biol. Chem. 2002, 277:19579-19584.
doi: 10.1074/jbc.M110993200 originally published online March 26, 2002

THE JOURNAL OF BIOLOGICAL CHEMISTRY
Vol. 277, No. 22, Issue of May 31, pp. 19579–19584, 2002
Printed in U.S.A.

Disruption of Mitochondrial β-Oxidation of Unsaturated Fatty Acids in the 3,2-*trans*-Enoyl-CoA Isomerase-deficient Mouse*

Received for publication, November 16, 2001, and in revised form, March 11, 2002
Published, JBC Papers in Press, March 26, 2002, DOI 10.1074/jbc.M110993200

Uwe Janssen and Wilhelm Stoffel‡

From the Laboratory of Molecular Neurosciences, Institute of Biochemistry, Faculty of Medicine, University of Cologne, Joseph-Stelzmannstrasse 52, D-50931 Cologne, Germany

Cellular energy metabolism is largely sustained by mitochondrial β-oxidation of saturated and unsaturated fatty acids. To study the role of unsaturated fatty acids in cellular lipid and energy metabolism we generated a null allelic mouse, deficient in 3,2-*trans*-enoyl-CoA isomerase (ECI) (*eci*$^{-/-}$ mouse). ECI is the link in mitochondrial β-oxidation of unsaturated and saturated fatty acids and essential for the complete degradation and for maximal energy yield. Mitochondrial β-oxidation of unsaturated fatty acids is interrupted in *eci*$^{-/-}$mice at the level of their respective 3-*cis*- or 3-*trans*-enoyl-CoA intermediates. Fasting *eci*$^{-/-}$ mice accumulate unsaturated fatty acyl groups in ester lipids and deposit large amounts of triglycerides in hepatocytes (steatosis). Gene expression studies revealed the induction of peroxisome proliferator-activated receptor activation in *eci*$^{-/-}$ mice together with peroxisomal β- and microsomal ω-oxidation enzymes. Combined peroxisomal β- and microsomal ω-oxidation of the 3-enoyl-CoA intermediates leads to a specific pattern of medium chain unsaturated dicarboxylic acids excreted in the urine in high concentration (dicarboxylic aciduria). The urinary dicarboxylate pattern is a reliable diagnostic marker of the ECI genetic defect. The *eci*$^{-/-}$ mouse might be a model of a yet undefined inborn mitochondrial β-oxidation disorder lacking the enzyme link that channels the intermediates of unsaturated fatty acids into the β-oxidation spiral of saturated fatty acids.

Long chain saturated and unsaturated (mono- and polyunsaturated) fatty acids comprising members of the ω-3 (α-linolenic), ω-6 (linoleic), and ω-9 (oleic acid) families occur almost equally as acyl groups of phospholipids and triglycerides. In phospholipids they are essential in the regulation of the fluidity of biological membranes. ω-3 and ω-6 polyunsaturated fatty acids are the precursors in eicosanoid synthesis (prostaglandins, prostacyclins, thromboxanes, and leukotrienes). As constituents of triglycerides, unsaturated fatty acids are a main energy source for muscle work.

Following the classical pathway of mitochondrial β-oxidation of unsaturated fatty acids with *cis* double bonds at odd-numbered C atoms, *e.g.* of oleic acid (18:1^{9}), linoleic acid (18:1^{9,12}), and α-linolenic acid (18:1^{9,12,15}), yields 3-*cis*-enoyl-CoA-intermediates. They are isomerized by the mitochondrial 3,2-*trans*-enoyl-CoA isomerase (ECI)[1] (EC 5.3.3.8) to their respective 2-*trans*-enoyl-CoA isomers, common substrates of enoyl-CoA hydratase of the β-oxidation cycle of saturated fatty acyl-CoA esters (1). *cis* double bonds at even C atoms yield 2-*trans*-4-*cis*-intermediates, which are reduced and isomerized by a mitochondrial NADPH-dependent 2,4-dienoyl-CoA reductase (EC 1.3.1.34) to their respective 3-*trans*-intermediates (2–4). Hydration to the D(−)-3-hydroxy derivative followed by epimerization by 3-hydroxyacyl-CoA epimerase (EC 5.1.2.3) is apparently an alternative but minor pathway. Likewise, another alternative pathway has been proposed, according to which a *cis*-5 double bond when encountered in the β-oxidation of an odd-numbered double bond in unsaturated fatty acids is removed through an NADPH-dependent reduction of 5-enoyl-CoA, possibly mediated by a 5-enoyl-CoA reductase (5). The enzyme, however, has neither been characterized on the protein level, nor has it been cloned. Its contribution to the overall mitochondrial β-oxidation of unsaturated fatty acids awaits further clarification.

According to the classical pathway of mitochondrial β-oxidation, all unsaturated fatty acids are channeled via their 3-*cis*- and/or 3-*trans*-enoyl-CoA isomers to their respective 2-*trans*-enoyl-CoA intermediates, which are regular intermediates of the β-oxidation spiral. Mitochondrial 3,2-*trans*-enoyl-CoA isomerase is the essential link between saturated and unsaturated β-oxidation. The peroxisomal trifunctional enzyme (pTFE) contains an isomerase subunit, which carries out the equivalent reaction when peroxisomal β-oxidation is challenged, *e.g.* by lipid-lowering drugs (6).

Mature ECI of mouse, rat, bovine, and man are 29-kDa soluble mitochondrial matrix proteins (7, 8). The cDNA-derived amino acid sequence of rodents encodes a 289-residue polypeptide (32 kDa) with a 28-residue N-terminal signal sequence, and that of human encodes a 302-residue ECI (33 kDa) with a 41-residue N-terminal signal sequence, which are processed to the 261-residue mature enzyme during mitochondrial import (9–11). The human *eci* locus has been assigned to chromosome 16p13.3 (12) and the mouse gene characterized (13).

A growing number of inborn errors of mitochondrial β-oxidation enzymes form a new class of metabolic diseases following the first description of the carnitine-palmitoyl transferase deficiency (14–17) and the molecular basis of several additional β-oxidation enzyme defects are awaiting clarification.

Common to these genetic defects is an impaired utilization of fatty acids as primary energy source. Starvation or increased energy requirement, particularly of newborns and children, causes severe hypoketotic hyperglycemia, elevated cellular and serum fatty acid concentrations, and enhanced ω-oxidation with medium chain length dicarboxylic acids as end products

* This work was supported by grants from the Fritz Thyssen Stiftung and the Deutsche Forschungsgemeinschaft. The costs of publication of this article were defrayed in part by the payment of page charges. This article must therefore be hereby marked "*advertisement*" in accordance with 18 U.S.C. Section 1734 solely to indicate this fact.

‡ To whom correspondence should be addressed. Tel.: 49-221-478-6881; Fax: 49-221-478-6882; E-mail: wilhelm.stoffel@uni-koeln.de.

[1] The abbreviations used are: ECI, 3,2-*trans*-enoyl-CoA isomerase; pTFE, peroxisomal trifunctional enzyme; PPAR, peroxisomal proliferator-activating receptor; SCAD, short chain acyl-CoA dehydrogenase; CYP 4A1, cytochrome P450 IVA1; RT, reverse transcription.

that are excreted in the urine.

We studied the function of mitochondrial β-oxidation of unsaturated fatty acids in cellular energy metabolism in a null allelic mouse model in which the key enzyme of mitochondrial β-oxidation of unsaturated fatty acids, ECI, has been disrupted by homologous recombination in mouse ES cells.

The complete ablation of *eci* in the mouse severely perturbs the metabolism of unsaturated fatty acids, particularly on short interval starvation. The fatty acid pattern of complex phospholipids is strongly altered. Saturated fatty acids become substituted by unsaturated fatty acids, and triglycerides massively accumulate in hepatocytes (steatosis). The lack of 3,2-*trans*-enoyl-CoA isomerase interrupts β-oxidation at the level of their 3-*cis*- or 3-*trans*-enoyl-CoA intermediates. They are further processed to specific medium chain saturated and unsaturated dicarboxylic acid end products and excreted into the urine. The urinary dicarboxylate pattern may serve as an unambiguous and valuable diagnostic tool in the diagnosis of the ECI genetic defect.

EXPERIMENTAL PROCEDURES

Construction of Replacement Vector—An 8-kb *Bam*HI fragment encoding exons III–VII from the mouse genomic phage clone λ-iso-8 described previously (13) was cloned into the *Bam*HI site of pBluescript SK+. The *neo* resistance gene, isolated as a *Xho*I/*Bam*HI fragment from the vector pMC1 *neo* poly(A) (Stratagene), was inserted by blunt end ligation into the *Sma*I site of exon IV (Fig. 1). The *Sma*I site of the vector was deleted by a *Sma*I/*Hin*cII restriction and blunt end religated. The 9.2-kb insert was isolated as a *Bam*HI fragment and cloned into the *Bam*HI site of the pIC19R-MC-I TK vector (18) at the 3′ end of the thymidine kinase box. 3-kb homologous ECI sequences flank the *neo* box in exon IV on each side with conserved exon sequences. The early stop of transcription by the *neo* box should yield an inactive, truncated gene product lacking amino acids 88–289.

Analysis of the Genotypes—Homologous integration of the insert leads to a *Bam*HI restriction fragment length polymorphism of genomic DNA of ES clones and of tail DNA, which was probed in Southern blot hybridization analysis (9.2-kb fragment; Fig. 1*D*) and PCR with the probes and primers indicated in Fig. 1*C*.

Homologous Recombination in E14 or R1 ES Cells and Generation of the eci$^{-/-}$ Mouse Line—ES cell lines E14 (129/Ola) and R1 (129/j × 129/sv-cp) were electroporated with the replacement vector pMIG-8TN (Fig. 1*A*). Cells were submitted to G418 and ganciclovir double selection. A targeting frequency of 2×10^{-7} and 1.7×10^{-7} for E14 and R1 cells, respectively, was observed. Blastocysts from C57/Bl6 and CD1 mice were used for cell transfer following established procedures (18, 19). One germ line chimeric mouse with R1 cell genetic background was obtained for further breeding to homozygosity. Genomic DNA of ES cells and tail biopsies was isolated as described previously.

RNA Analysis—Total RNA from ES cells and different mouse organs was isolated by the acid guanidinium/phenol/chloroform method (17, 20). Southern and Northern blot hybridization analysis was carried out following established procedures (21). Oligonucleotide primers indicated in Fig. 1 were used for the proof of homologous recombination by polymerase chain reaction (PCR): NeoN-3′s, 5′-gcgcatcgccttctatcgccttctgacga-3′; MisoN-3′as, 5′-acatatgtggcagccgtaggttagcccttа-3′; ExIVs, 5′-ctcctgagccatttcccaggatttggtcct-3′, ExIVas, 5′-tgttggaacgtagagtctcagccacagct-3′ for probing the exon IV domain. Annealing temperature was 70 °C, for 20–35 cycles.

ECI Enzyme Assay and Lipid Analyses—The enzymatic activity was measured with 3-*cis*-dodecanoyl-CoA as substrate as described elsewhere (1). Total lipids were extracted as described (22) and lipid classes separated by high performance thin layer chromatography Silica gel 60 plates: neutral lipids in the solvent system diisopropyl ether-acetic acid (96:4, v/v) and hexane:diethylether:acidic acid (90:10:1 v/v/v) and total lipids chloroform:methanol:water (65:25:4, v/v/v). Plates were sprayed with 50% H_2SO_4 and charred at 120 °C. Fatty acids were identified and quantified as methyl esters by gas chromatography using a DB-225 capillary column (30 m) with margerinic acid and reference compounds as internal standard. Fatty acid methyl esters were identified by combined gas liquid chromatography-mass spectrometry using a Permabond FFAP capillary column and the mass spectrometer Hewlett Packard model 5989A. A temperature gradient program was run between 100 and 240 °C; 10 °C/min; 15 min at 240 °C.

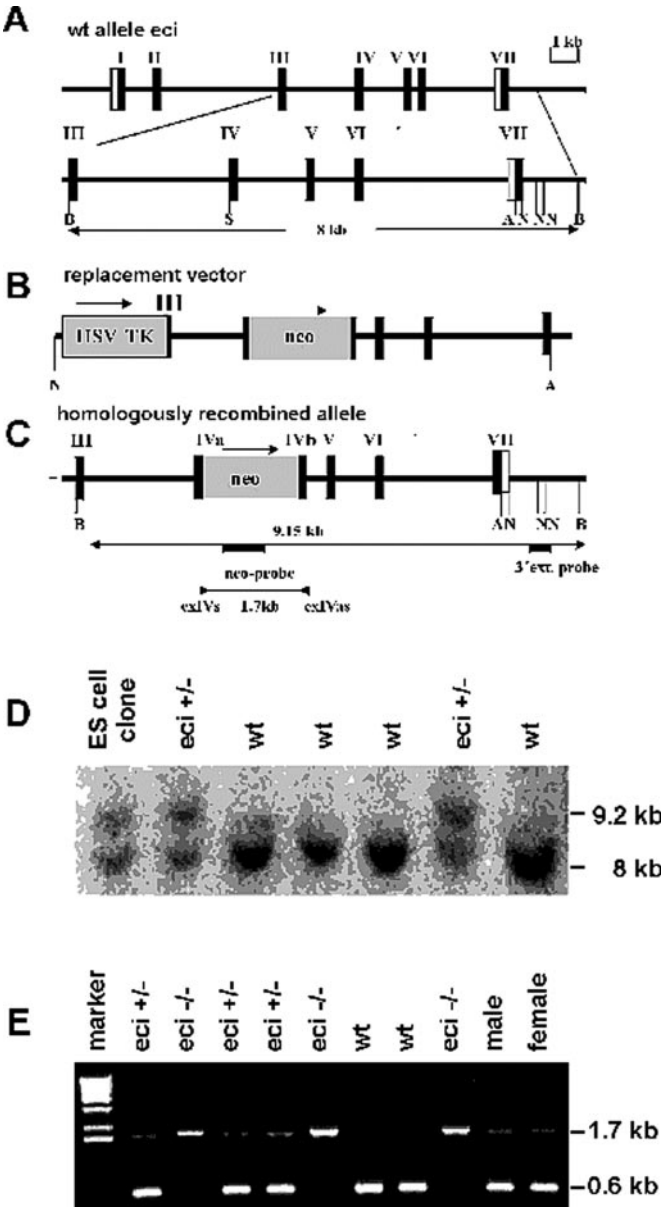

FIG. 1. *A*, organization of the *eci* allele of the mouse and of the zoomed 8-kb *Bam*HI fragment used for the construction of the *eci* replacement vector. *B*, replacement vector MIG-8TN containing the HSV-tk gene, 5′-flanking exon III, exon IV interrupted by the *neo* resistance gene, and exons V–VII. *C*, targeted mutated *eci* locus in ES cells. The sites of the primers NeoN-3′s and MIsoN-3′as and ExIVs and ExIVas, as well as the external 3′ probe and internal *neo* probe, are indicated. *D*, Southern blot hybridization analysis of *Bam*HI restricted genomic DNA of ES cell clone, *wt*, and heterozygous siblings of F1 generation. *E*, PCR analysis of hetero- (*eci*$^{+/-}$) and homozygous (*eci*$^{-/-}$) F2 generation with primers ExIVs and ExIVas. The 1.7-kb fragment represents the wild type (*wt*) fragment (860 bp) extended by the *neo* gene sequence (1.1 kb).

RESULTS

Generation Genotyping of the ECI-deficient Mouse—The 8-kb BamH1 mouse genomic fragment in the replacement vector contained exons III–VII of *eci* (Fig. 1*A*). The *neo* gene was inserted into a unique *Sma*I restriction site in exon IV, which disrupted the transcription of the homologously recombined allele. The unique *Avr*II site in exon VII was used for linearization of the vector for electroporation (Fig. 1*B*). The targeted mutated *eci* locus is depicted in Fig. 1*C*.

Electroporation of E14 (129/ola) and R1 (129/j × 129/sv-cp) embryonic stem cells, negative/positive selection, blastocyst injection, and crossing chimeric mice to homozygosity were car-

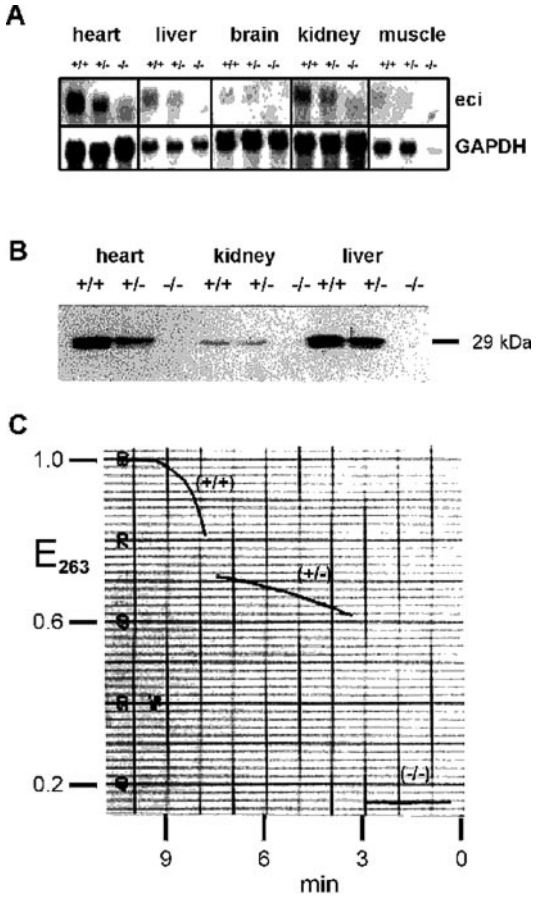

FIG. 2. *A*, ECI expression in heart, liver, brain, kidney, and muscle of *wt*, $eci^{+/-}$, and $eci^{-/-}$ mice visualized by Northern blot hybridization using a 650-bp *Nco*I fragment of mouse ECI cDNA probes. Glyceraldehyde-3-phosphate dehydrogenase (*GAPDH*) mRNA was used as internal standard. *B*, Western blot analysis of tissue homogenates of *wt*, $eci^{+/-}$, and $eci^{-/-}$ mice with anti-rat isomerase polyclonal antibodies. *C*, enzyme activity of heat-treated, undiluted liver mitochondrial lysate of $eci^{-/-}$ (*a*), 5-fold diluted (*b*), and undiluted (*c*) liver mitochondrial lysate of *wt* mice. The 263-nm absorption monitors the shift of the double bond from the 3-position to the 2-position.

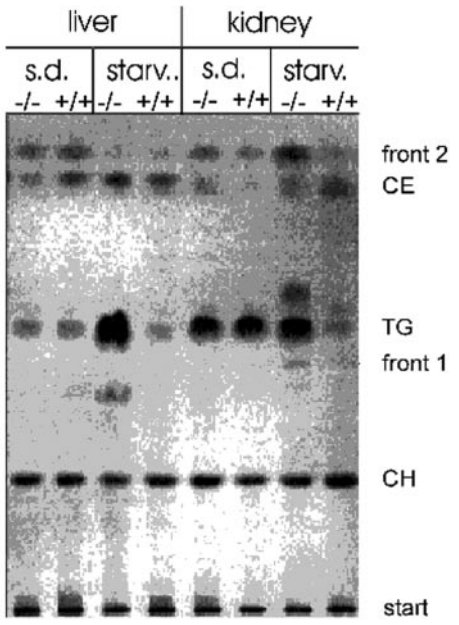

FIG. 3. **Thin layer chromatographic separation of total lipids of liver and kidney of *wt* and $eci^{-/-}$ mice on standard diet (*s.d.*) and after starvation (*starv*) for 48 h.** *1*, solvent system was diisopropyl ether:acetic acid (96:4, v/v); *2*, solvent system was hexane:diethyl ether:acetic acid (90:10:1, v/v/v). TLC plates were charred with 50% sulfuric acid and charred at 120 °C for visualization of lipid bands. *CH*, cholesterol; *TG*, triglycerides; *CE*, cholesterol esters.

ried out following established procedures (18). Southern blot hybridization analysis of *Bam*HI-restricted ES cell clones and tail DNA of *wt*, $eci^{+/-}$, and $eci^{-/-}$ progeny (Fig. 1*D*) revealed the expected restriction fragment length polymorphism, a 9.2-kb *Bam*HI fragment from the mutant and a 8-kb fragment from the *wt* allele, indicative of the homologous recombination event in $eci^{+/-}$ and $eci^{-/-}$ progeny. PCR analysis with exon-specific oligonucleotides as primers proved that exon IV and the *neo* box had been spliced out (Fig. 1*E*).

Analysis of the ECI-deficient Phenotype—Gene expression of *wt*, $eci^{+/-}$, and $eci^{-/-}$ progeny was studied on the RNA, enzyme protein, and enzyme activity level. The *wt* mRNA transcript is 1.3 kb (8). *wt* and $eci^{+/-}$ mice showed the expected 1.3-kb transcript in liver, heart, kidney, and muscle and was weakly expressed in brain. The *eci* signal was more than 50% reduced in the $eci^{+/-}$ mouse (Fig. 2). The $eci^{-/-}$ mRNA carried a 147-bp deletion (exon IV) and encodes 212 of 261 amino acid residues of the mature ECI. The low intensity of the Northern blot signal suggested a reduced stability of the transcripts (Fig. 2). Western blot analysis of tissue extracts of heart, kidney, and liver failed to detect the immunoreactive 29-kDa ECI or derived peptide fragments. Additionally, the sensitive optical assay (263 nm absorbance) revealed the complete lack of ECI activity as expected from the missing ECI polypeptide (Fig. 2*C*).

These results proved that we had generated a ECI-deficient mouse line. Surprisingly, the ECI-deficient mice developed inconspicuously, were fertile, and had a normal life span. This agrees well with β-oxidation defects in human newborns, *e.g.* short chain acyl-CoA dehydrogenase (SCAD) deficiency. Affected individuals also develop a dramatic phenotype only after reduced carbohydrate supply, starvation, or physical stress.

Starvation Changes Rapidly the Fatty Acid Pattern of Total Lipids in $eci^{-/-}$ Mice—We studied the impact of ECI deficiency on lipid and fatty acid metabolism during short starvation intervals.

Total lipids of liver and kidney of *wt* and $eci^{-/-}$ mice, which were starved for 24 and 48 h, were separated by thin layer chromatography (TLC) for quantitative analysis using the ImageQuant software (Fig. 3). Under standard diet the ratio of triglyceride/cholesterol in the liver of both genotypes, *wt* and $eci^{-/-}$, was ~1 and in the kidney, 1.6 and 1.4, respectively. After a 48-h fasting period, the triglyceride/cholesterol ratio in total lipids of liver of $eci^{-/-}$ mice increased to 3.6 and in total lipids of kidney to 1.5, but decreased to 0.5 in liver and 0.3 in kidney of *wt* mice.

Aliquots of total lipid of liver and kidney of *wt* and $eci^{-/-}$ mice on normal and fasting diet, respectively, were transesterified, separated, and quantified by gas liquid chromatography. $eci^{-/-}$ and *wt* mice on standard diet showed a similar fatty acid composition in liver and kidney lipids (Fig. 4*A*), but fasting for 48 h reduced unsaturated fatty acids of triglycerides, whereas a strongly enhanced acylation of liver and kidney lipids of $eci^{-/-}$ mice occurred with an accumulation of all unsaturated fatty acids (Fig. 4*B*). Only the 20:4 concentration remained unchanged. Table I summarizes the quantitation of the increased ratio of unsaturated *versus* saturated fatty acyl residues in ester lipids of liver.

Urinary Metabolites of Fatty Acids in the ECI-deficient Mouse—We collected the urine of cohorts of four *wt* and $eci^{-/-}$ mice, respectively, which were fed a standard diet over a period of 20 h as control and subsequently starved for 48 h. Samples

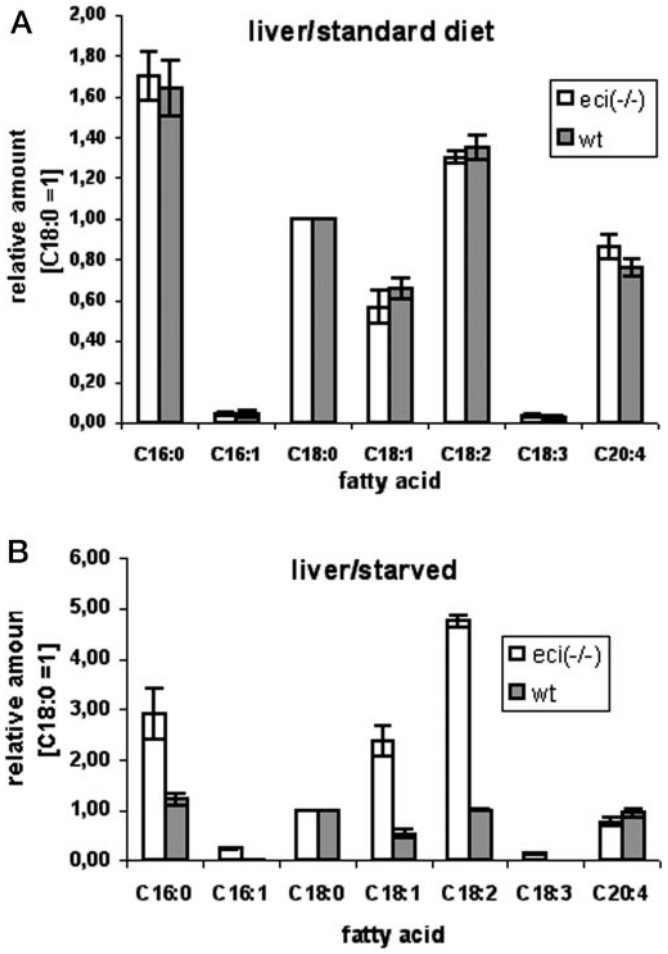

FIG. 4. **Shift of fatty acyl substitution in ester lipids (mostly triglycerides) of liver and kidney toward unsaturated fatty acids.** Figure shows fatty acid composition of total lipids of liver and kidney of *wt* and *eci*$^{-/-}$ mice on standard diet (*A*) and after 48-h starvation (*B*). Methyl stearate (18:0) was chosen as standard for the normalization. *Open bars*, homozygous mice; *filled bars*, *wt* mice. Bars represent the average value of five *wt* and homozygous mice of same genotype and age with the quantitation of two runs of each sample.

TABLE I
Shift of ester fatty acyl residues to unsaturated substituents (oleic 18:1, linoleic 18:2, and linolenic acid 18:3)

Liver	Starvation		Ratio[a]
	eci$^{-/-}$	wt	
C16:0	2.91	1.22	2.40
C16:1	0.24	0.03	9.25
C18:0	1.00	1.00	1.00
C18:1	2.39	0.53	4.53
C18:2	4.75	1.01	4.72
C18:3	0.14	0.00	
C20:4	0.77	0.94	0.81

[a] Calculated from mean values of Fig. 4.

were acidified, margerinic acid (19:0) added as internal standard, and fatty acids extracted and esterified for gas liquid chromatography-mass spectrometry analysis. Fatty acid structures were assigned using reference compounds for comparison with reference spectra from the spectrum library. The *eci*$^{-/-}$ mouse excreted severalfold higher concentrations of C6, C7, and C8 normal, monoenedioic, and dienedioic acids. The most significant indicator molecule in *eci*$^{-/-}$ urine, hex-3-*cis*-ene-1,6-dioic acid derived from oleic acid, was present in a 30-fold higher concentration than in *wt* urine (Table II).

Induction of Enzymes of Extramitochondrial Fatty Acid Oxidation—We studied the regulation of the expression of enzymes most likely involved in the enzymatic transformation of the 3,2-*trans*-enoyl-CoA intermediates. These included pTFE, which contains the extramitochondrial 3,2-*trans*-enoyl-CoA isomerase activity and the key enzyme of microsomal ω-oxidation, cytochrome P450 IVA1 (CYP 4A1). Hybridization probes for Northern blot analysis were obtained by RT-PCR using PCR primers derived from published cDNA sequences, a 527-bp fragment (bp 1664–2190) of the pTFE cDNA (23) and a 607-bp fragment of the CYP 4A1 cDNA (24).

Fig. 5 (*A* and *B*) summarizes the results of the Northern blot hybridization and its quantification by phosphorimaging.

In *eci*$^{-/-}$ and *wt* mice, the expression of pTFE and CYP 4A1 was minute in liver and kidney under standard dietary conditions. After a 24- and 48-h fasting period, respectively, a strong induction of the expression of pTFE and an even more dramatic increase of CYP 4A1 in ECI-deficient mice was observed. Fasting significantly enhanced the expression of peroxisomal proliferator-activating receptor (PPAR)α only in *eci*$^{-/-}$ mice within the first 24 h but not in *wt* mice.

In kidney of *wt* mice, pTFE expression remained unchanged during fasting, but pTFE expression in *eci*$^{-/-}$ mice increased ~2-fold after 48 h fasting.

DISCUSSION

This report describes the generation and characterization of the first mouse model that addresses the catabolism of unsaturated fatty acids. ECI is the enzyme that links unsaturated and saturated fatty acid mitochondrial β-oxidation essential for the complete degradation of unsaturated fatty acids for optimal energy yield. In the *eci*$^{-/-}$ mouse, mitochondrial unsaturated fatty acid β-oxidation is interrupted at the stage of their 3-*cis*- or 3-*trans*-enoyl-CoA intermediates. *eci*$^{-/-}$ mice show no obvious phenotypic differences under normal physiological conditions. However, like patients affected by mitochondrial β-oxidation defects of saturated fatty acids (15), the *eci*$^{-/-}$mouse develops pathological symptoms as soon as energy supply becomes dependent on mitochondrial fatty acids oxidation, *e.g.* in hypoglycemic state during fasting periods.

In general two independent β-oxidation systems, a mitochondrial and a peroxisomal, are involved in the degradation of saturated and unsaturated fatty acids. Peroxisomes catalyze fatty acid oxidation in a reaction sequence similar to the mitochondrial β-oxidation spiral, although only through two to five cycles for fatty acyl chain shortening. Unlike in mitochondria the reduction equivalents released in the peroxisomal β-oxidation cannot be utilized by oxidative phosphorylation. Therefore, the energy production is only minor and contributes under prolonged fasting conditions to total cellular fatty acid oxidation no more than 20% (25, 26). Therefore, ECI is essential for the energy supply by mitochondrial β-oxidation from unsaturated fatty acids. Their abundance defines them as essential metabolic fuel for the energy supply by mitochondrial β-oxidation. The important function of 3,2-*trans*-enoyl-CoA isomerase in the complete mitochondrial degradation of unsaturated fatty acids to acetyl-CoA is obvious.

Mitochondrial ECI and the isomerase subunit of pTFE are equivalent in their catalytic function. The mouse and human ECI gene organization (11, 12) and of pTFE consist of seven exons. Exon I–V of *ptfe* encode the peroxisomal isomerase-hydratase activity with 25% identity to the *heci* (27). However, the exon/intron positions of mitochondrial *eci* and peroxisomal rn*tfe* show no similarity, which indicates the independent evolutionary development of the mitochondrial and peroxisomal β-oxidation to acetyl-CoA.

The important question arose of whether in the *eci*$^{-/-}$ mouse mutant peroxisomal β-oxidation can compensate for the deficiency of mitochondrial β-oxidation and carry out the complete

TABLE II
Dicarboxylic aciduria in eci$^{-/-}$ mice

Dicarboxylic acid pattern in urine of cohorts (5 animals/cohort) of wild type and homozygous ECI-deficient mice of same genotype, age (2–3 months), sex, and approximate weight on standard diet and under fasting conditions, collected during 24-h fasting (with free access to water). Mean values of three experiments. RT, retention time; ND not detected. All values were normalized to urinary creatinine.

Dicarboxylic acids[a]	RT	Standard diet		Starvation	
		eci$^{-/-}$	*wt*	*eci*$^{-/-}$	*wt*
DC6	5.52	13.7 ± 0.5	4.9 ± 0.4	73.3 ± 2.5	13.0 ± 1.5
c3DC6	6.27	2.1 ± 0.3	ND	44.1 ± 2.3	1.4 ± 0.4
t3DC6	6.50	1.8 ± 0.4	ND	16.1 ± 0.6	4.5 ± 0.7
DC7	6.55	3.8 ± 0.4	4.7 ± 0.5	3.6 ± 0.4	1.6 ± 0.2
DC7ene	7.04	1.6 ± 0.5	ND	16.1 ± 1.4	1.9 ± 0.3
DC8	7.59	1.3 ± 0.3	1.8 ± 0.4	5.8 ± 1.2	3.6 ± 0.4
c3DC8ene[b]	7.87	5.3 ± 1.1	4.8 ± 0.9	77.6 ± 3.4	16.6 ± 1.2
t3DC8ene[b]	7.97	ND	ND	10.7 ± 0.8	ND
DC8diene	10.32	ND	ND	37.8 ± 2.4	8.4 ± 0.8

[a] DC6, hexane-1,6-dioic acid; c3DC6, hex-3-*cis*-ene-1,6-dioic acid; t3DC6, hex-3-*trans*-ene-1,6-dioic acid; DC7, heptane-1,7-dioic acid; DC7ene, heptene-1,7-dioic acid; DC8, octane-1,8-dioic acid; c3DC8ene, oct-3-*cis*-ene-1,8-dioic acid; t3DC8ene, oct-3-*trans*-ene-1,8-dioic acid; DC8diene, octadiene-1,8-dioic acid.
[b] The stereoisomerism has been deduced by analogy from the retention times of corresponding c3DC6 and t3DC6 homologs.

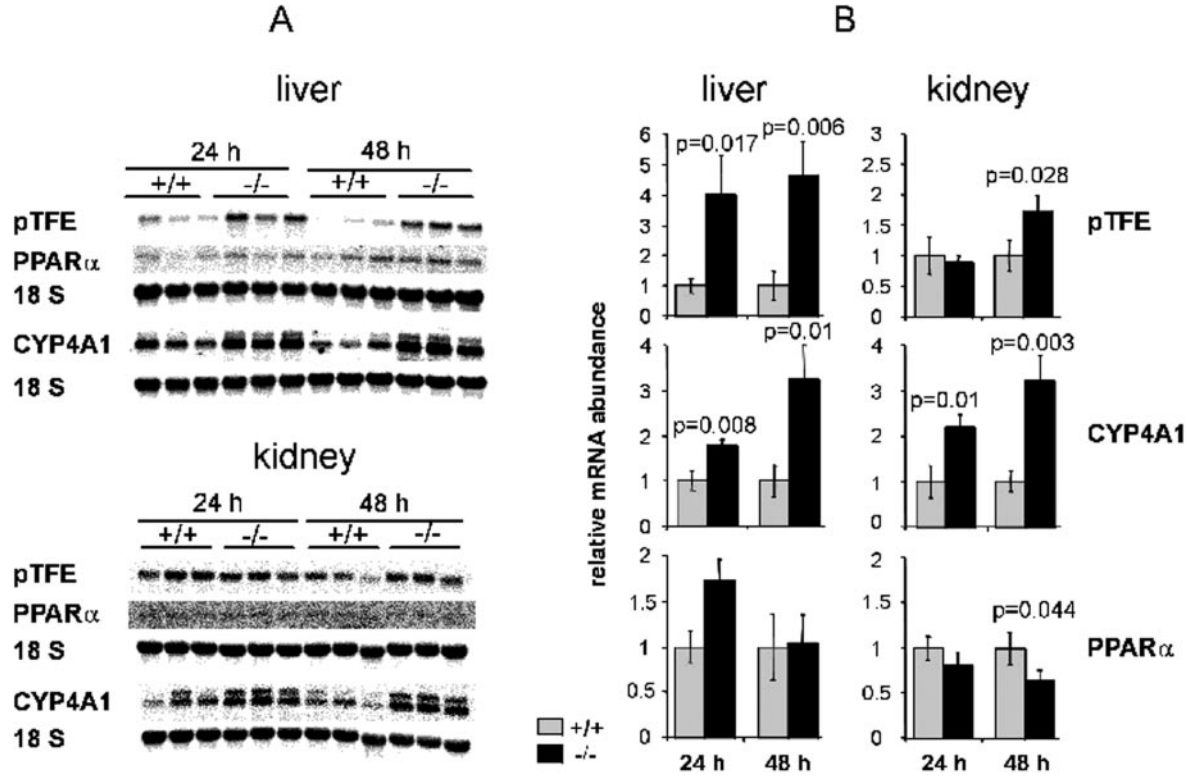

FIG. 5. *A*, expression of pTFE and CYP 4A1 in heart, liver, and kidney of *wt* (+/+) and homozygous (−/−) *eci* mice, on standard diet and after 24 h of starvation: Northern blot hybridization analysis. The following probes were used to quantify the expression of their relevant mRNAs: 527-bp RT-PCR fragment of rat pTFE cDNA, 607-bp RT-PCR fragment of rat CYP 4A1 cDNA, and 650-bp *Nco*I fragment of rat ECI cDNA. *B*, graphic presentation of densitometry of Northern blot signals.

degradation of the accumulating 3-*cis*- and 3-*trans*-isomeric intermediates of unsaturated fatty acid β-oxidation.

Surprisingly, *eci*$^{-/-}$ mice are viable, fertile, and phenotypically indistinguishable from *wt* mice as long as they are unchallenged by metabolic stress. The genotypes of the siblings of heterozygous crosses (*eci*$^{+/-}$ mice) followed the Mendelian law and excluded an influence of ECI deficiency on embryonic development.

Most human mitochondrial β-oxidation enzyme defects described thus far are involved in mitochondrial β-oxidation of saturated fatty acids. Affected individuals develop a pathological phenotype only when an enhanced energy requirement must be covered by mitochondrial fatty acid β-oxidation, *e.g.* during prolonged fasting (29).

Our ECI-deficient mice show three characteristic features. 1) A massive accumulation of neutral lipids, mainly triglycerides, occurs in liver and kidney upon short fasting conditions (Fig. 3). 2) Starvation induces hormonal activation of adipose tissue triglyceride lipase, elevates free fatty acid concentration in serum, and enhances mitochondrial and extra mitochondrial fatty acid oxidation. The activation of the hormone-sensitive adipose tissue triglyceride lipase releases long chain unsaturated fatty acids selectively from fat cell triglycerides (28). Liver of *eci*$^{-/-}$ mice is supplied with these unsaturated long chain fatty acids. They are utilized for the synthesis of ester lipids (triglyceride and phospholipids). Because of their impaired mitochondrial β-oxidation, they are mainly stored as cytosolic triglycerides in hepatocytes, as documented in the TLC analysis of *eci*$^{-/-}$ liver and kidney lipids (Fig. 3).

Triglyceride storage in the liver described here for the *eci*$^{-/-}$

mouse has also been observed in SCAD-deficient mice (29). Both the unchallenged $eci^{-/-}$ and the $scad^{-/-}$ mouse are clinically asymptomatic, different from the SCAD deficiency in human, characterized by severe clinical symptoms.

3) PPAR isoforms are activated by free fatty acids and accumulating metabolites (30, 31). Upon starvation the $eci^{-/-}$ mouse rapidly develops a disrupted lipid metabolism. PPARα expression is up-regulated within the first 24 h, associated with a strongly enhanced expression of microsomal cytochrome P450 A1 and the peroxisomal β-oxidation enzymes, as documented here for the gene expression of CYP 4A1 and pTFE in the liver (Fig. 5).

In $eci^{-/-}$ mice unsaturated fatty acid intermediates become substrates of these enzymes. As a consequence large amounts of saturated and unsaturated dicarboxylic acids are excreted in the urine, leading to a characteristic urinary dicarboxylate pattern in which hex-3-*cis*-ene-1,6-dioic acid is a dominant end product exceeding that of wild type control mice 30-fold. Because of the abundance of oleic acid among unsaturated fatty acids in phospholipids and triglycerides, ECI deficiency leads to a halt of the regular β-oxidation of oleic acid on the dodec-3-*cis*-enoyl-CoA level, which becomes the substrate of the P450-dependent microsomal ω-oxidation. Dodec-3- and 9-*cis*-ene-1,6-dioic acid is then activated by the microsomal dicarboxylyl-CoA synthase (32) and further degraded either in mitochondria or in peroxisomes to hex-3-*cis*-ene-1,6-dicarboxylic acid. Octadi-2,5-*cis*-ene-1,8-dioic acid is another characteristic and abundant degradation product, which is derived from linoleic acid (18:$2^{9,12}$). Degradation of octadi-2,5-*cis*-ene-1,8-dioic acids via peroxisomal β-oxidation complex (hydratase to the D-3-hydroxy- and epimerase to the L-3-hydroxy-intermediate, dehydrogenase, and thiolase) might further increase the hex-3-*cis*-ene-1,6-dioic acid concentration in the urinary dicarboxylic acid pattern.

All isomeric hexene, octene, octadiene, and decadiene dioic acids have been identified and characterized by gas liquid chromatography except the *cis*-/*trans*-isomerism of the latter. Triglyceride storage and dicarboxylic aciduria upon fasting as described above is a phenotypic sign, which is shared between the $eci^{-/-}$ mouse and the human inborn error SCAD deficiency. In SCAD deficiency starvation also causes a massive increase in urinary ethylmalonate and methylsuccinate as specific dicarboxylate metabolites, which results from ω-oxidation of incompletely β-oxidized saturated fatty acids.

The $eci^{-/-}$ mouse model deficient in the 3,2-*trans*-enoyl-CoA isomerase, which links mitochondrial β-oxidation of saturated and unsaturated fatty acids, furthers our understanding of the role of unsaturated fatty acids in energy metabolism in response to normal and fasting conditions. The molecular pathology and the analysis of its phenotype has provided specific diagnostic tools. The $eci^{-/-}$ mouse mutant might prove to be a valuable mimicry of human ECI deficiency and facilitate the discovery of the equivalent human inherited disease in the pool of hitherto unknown mitochondrial fatty acid β-oxidation defects observed in new born and infants. The mouse model might also be useful in the development of dietary therapeutic strategies.

REFERENCES

1. Stoffel, W., Ditzer, R., and Caesar, H. (1964) *Hoppe Seylers Z. Physiol. Chem.* **339,** 167–181
2. Kunau, W. H., and Dommes, P. (1978) *Eur. J. Biochem.* **91,** 533–544
3. Luo, M. J., Smeland, T. E., Shoukry, K., and Schulz, H. (1994) *J. Biol. Chem.* **269,** 2384–2388
4. Koivuranta, K. T., Hakkola, E. H., and Hiltunen, J. K. (1994) *Biochem. J.* **304,** 787–789
5. Tserng, K., Y., and Jin, S., J. (1991) *J. Biol. Chem.* **266,** 11614–11620
6. Novikov, D. K., Koivuranta, K. T., Helander, H. M., Filppula, S. A., Yagi, A. I., Qin, Y. M., and Hiltunen, K. J. (1999) *Adv. Exp. Med. Biol.* **466,** 301–309
7. Stoffel, W., and Grol, M. (1978) *Hoppe Seylers Z. Physiol. Chem.* **359,** 1777–1782
8. Euler-Bertram, S., and Stoffel, W. (1990) *Biol. Chem. Hoppe Seyler* **371,** 603–610
9. Muller-Newen, G., and Stoffel, W. (1991) *Biol. Chem. Hoppe Seyler* **372,** 613–624
10. Muller-Newen, G., Janssen, U., and Stoffel, W. (1995) *Eur. J. Biochem.* **228,** 68–73
11. Muller-Newen, G., and Stoffel, W. (1993) *Biochemistry* **32,** 11405–11412
12. Janssen, U., Fink, T., Lichter, P., and Stoffel, W. (1994) *Genomics* **23,** 223–228
13. Stoffel, W., Duker, M., and Hofmann, K. (1993) *FEBS Lett.* **333,** 119–122
14. Bennett, M. J. (1990) *Ann. Clin. Biochem.* **27,** 519–531
15. Di Mauro, S., and Di Mauro, P. M. (1973) *Science* **182,** 929–931
16. Amendt, B. A., Greene, C., Sweetman, L., Cloherty, J., Shih, V., Moon, A., Teel, L., and Rhead, W. J. (1987) *J. Clin. Invest.* **79,** 1303–1309
17. Wanders, R. J., IJlst, L., Poggi, F., Bonnefont, J. P., Munnich, A., Brivet, M., Rabier, D., and Saudubray, J. M. (1992) *Biochem. Biophys. Res. Commun.* **188,** 1139–1145
18. Bradley, A. (1987) *Production and Analysis of Chimeric Mice*, pp. 113–151, IRL Press, Oxford
19. Hogan, B., Costantini, F., and Lacy, E. (eds) (1986) *Manipulating the Mouse Embryo*, Cold Spring Harbor Laboratory, Cold Spring Harbor, NY
20. Chomczynski, P., and Sacchi, N. (1987) *Anal. Biochem.* **162,** 156–159
21. Sambrook, J., Fritsch, E. F., and Maniatis, T. (1989) *Molecular Cloning: A Laboratory Manual,* 2nd Ed, Cold Spring Harbor Laboratory, Cold Spring Harbor, NY
22. Bligh, E. G., and Dyer, W. J. (1959) *Can. J. Biochem. Physiol.* **37,** 911–917
23. Osumi, T., Ishii, N., Hijikata, M., Kamijo, K., Ozasa, H., Furuta, S., Miyazawa, S., Kondo, K., Inoue, K., Kagamiyama, H., and Hashimoto, T. (1985) *J. Biol. Chem.* **260,** 8905–8910
24. Hardwick, J. P., Song, B. J., Huberman, E., and Gonzalez, F. J. (1987) *J. Biol. Chem.* **262,** 801–810
25. Krahling, J. B., Gee, R., Murphy, P. A., Kirk, J. R., and Tolbert, N. E. (1978) *Biochem. Biophys. Res. Commun.* **82,** 136–141
26. Lazarow, P. B., and De Duve, C. (1976) *Proc. Natl. Acad. Sci. U. S. A.* **73,** 2043–2046
27. Ishii, N., Hijikata, M., Osumi, T., and Hashimoto, T. (1987) *J. Biol. Chem.* **262,** 8144–8150
28. Raclot, T., and Groscolas, R. (1995) *J. Lipid Res.* **36,** 2164–2173
29. Wood, P. A., Amendt, B. A., Rhead, W. J., Millington, D. S., Inoue, F., and Armstrong, D. (1989) *Pediatr. Res.* **25,** 38–43
30. Tontonoz, P., Hu, E., and Spiegelman, B. M. (1995) *Curr. Opin. Genet. Dev.* **5,** 571–576
31. Vidal-Puig, A., Jimenez-Linan, M., Lowell, B. B., Hamann, A., Hu, E., Spiegelman, B., Flier, J. S., and Moller, D. E. (1996) *J. Clin. Invest.* **97,** 2553–2561
32. Vamecq, J., de Hoffmann, E., and Van Hoof, F. (1985) *Biochem. J.* **230,** 683–693